

Contents lists available at ScienceDirect

Water Research

journal homepage: www.elsevier.com/locate/watres





Spatiotemporal analysis of fluorescent dissolved organic matter to identify the impacts of failing sewer infrastructure in urban streams

Jahir A. Batista-Andrade, Erick Diaz, Diego Iglesias Vega, Ethan Hain, Michael R. Rose, Lee Blaney *

Department of Chemical, Biochemical, and Environmental Engineering, University of Maryland Baltimore County, 1000 Hilltop Circle, Engineering 314, Baltimore, MD 21250. United States

ARTICLE INFO

Keywords:
Dissolved organic matter
Fluorescence
Sewer exfiltration
Sanitary sewer overflow
Septic system
Excitation-emission matrix

ABSTRACT

Failing sewer infrastructure introduces raw wastewater into streams. We used fluorescence excitation-emission matrix (EEM) spectroscopy and parallel factor analysis (PARAFAC) to track hotspots of raw wastewater in low- and medium-order urban streams that do not receive wastewater effluent but are impacted by sanitary sewer overflows, septic systems, and sewer exfiltration. After analyzing 296 surface water samples from 27 sites in two watersheds over a one-year period, we proposed that the (i) area-normalized ratio of soluble microbial product-like to humic acid-like fluorescence (R4/R5 \geq 0.85) and (ii) ratio of EEM-PARAFAC components with tryptophan-like and fulvic acid-like fluorescence (C4/C3 \geq 1.45) could distinguish when and where untreated wastewater is introduced to urban streams. The proposed ratios were validated by co-detection of contaminants of emerging concern, such as sucralose, antibiotics, and UV filters, at concentrations as high as 1354, 108, and $212 \, \mathrm{ng \, L}^{-1}$, respectively. Based on the aggregate data, we identified three sites in rural/suburban areas that were impacted by septic systems and ten sites in urban sections affected by sanitary sewer overflows and/or sewer exfiltration. Moreover, the ratiometric C4/C3 and R4/R5 parameters were immune to dilution effects caused by rain events. Impacts on upstream sites were mostly identified in spring and early summer, but urban hotspots occurred in almost every month. These findings confirmed the potential for EEM-PARAFAC-based wastewater indicators as a quick, easy, cost-effective, and scalable technique to screen for failing sewer infrastructure in loworder streams.

1. Introduction

Sanitary sewer overflows (SSOs), sewer exfiltration, and failing septic systems are common occurrences in urban areas with aging infrastructure and result in the introduction of raw wastewater to the environment, threatening ecological and public health (Ogidan and Giacomoni, 2016; US EPA, 2022). These issues occur due to failures in the wastewater collection system stemming from substandard construction materials, insufficient maintenance budgets, and logistical difficulties involved with replacement of aging infrastructure (Sercu et al., 2011). The risk of SSOs increases with precipitation events, flooding, and improper disposal of fats, oils, grease, and "flushable" wipes (Ashley et al., 2000; Durukan and Karadagli, 2019; Jagai et al., 2017; Sercu et al., 2011). Wastewater conveyance efficiencies have been documented for select locations. For example, the average efficiency of sewer infrastructure in 70 Chinese megacities was determined to be

76%, meaning 24% of wastewater was discharged without treatment (Wu et al., 2018). The United States Environmental Protection Agency (US EPA) estimated 23,000–75,000 SSOs per year, representing a loss of 3–10 billion gallons of raw wastewater (US EPA, 2022). These events directly introduce pathogens, primary pollutants (e.g., carbon, nitrogen, phosphorus), and contaminants of emerging concern (CECs), such as antibiotics, hormones, and UV filters that raise antimicrobial resistance (Berendonk et al., 2015) and endocrine disruption (de Cock and van de Bor, 2014) concerns, into urban and suburban streams.

Some cities provide transparent data about SSOs. For example, Baltimore City (USA) maintains a publicly accessible, web-based dashboard (Baltimore City, 2020). Tracking sewer leaks, however, is a major challenge in urban areas because exfiltration occurs underground and is not easily identified or quantified. To assess the influence of failing sewer infrastructure on water quality, previous efforts have attempted to estimate the location and the quantity of wastewater lost through sewer

E-mail address: blaney@umbc.edu (L. Blaney).

^{*} Corresponding author.

exfiltration and SSOs via groundwater modeling (Karpf and Krebs, 2011; Roldin et al., 2012; Thorndahl et al., 2016) and tracer studies with inorganics (Rieckermann et al., 2007) and fluorescent dyes (Sercu et al., 2011). These strategies require extensive groundwater, hydrogeological, and wastewater datasets that contain high uncertainty (Rutsch et al., 2006). Furthermore, the logistical complexities of large-scale tracer studies inhibit adoption especially in low-order streams, which are more vulnerable to the impacts of failing sewer infrastructure. To address these knowledge gaps, we propose spatiotemporal analysis of the dissolved organic matter (DOM) in urban streams as a quick, easy, and economical strategy to screen for raw wastewater.

Sewer exfiltration, SSOs, and septic systems introduce wastewaterderived DOM into urban streams. DOM is a complex mixture of carbohydrates, proteins, soluble microbial products, fulvic and humic substances, and other small molecules (Hudson et al., 2007). Previous research has shown that the fluorescence characteristics of wastewater-derived DOM are different than those of "natural" DOM stemming from plant and animal decay (Barbosa et al., 2018; Retelletti Brogi et al., 2019). Excitation-emission matrix (EEM) fluorescence spectroscopy has become a powerful tool to characterize the source and composition of fluorescent DOM (FDOM) in municipal wastewater (Guo et al., 2010), surface water (Singh et al., 2010), groundwater (Lapworth et al., 2008), and marine systems (Gonçalves-Araujo et al., 2016). Characterization and monitoring of FDOM could, therefore, provide an alternative strategy to understand the impacts of sewer exfiltration, septic systems, and SSOs on water quality in both the headwaters and also downstream sections of urban streams that do not receive wastewater effluent.

Chen et al. (2003) established five major fluorescence regions in EEMs: (1) tyrosine-like; (2) tryptophan-like; (3) fulvic acid-like; (4) soluble microbial product-like; and, (5) humic acid-like (Fig. S1). Baker (2001) measured FDOM in six English rivers and concluded that sites impacted by wastewater effluent exhibited higher tryptophan-like and fulvic acid-like fluorescence than upstream sites. The regional fluorescence volumes can be integrated to facilitate quantitative analysis of FDOM composition. Yang et al. (2013) reported that the cumulative volumes of aromatic protein-like (Regions 1 and 2) and soluble microbial product-like (Region 4) fluorescence were directly correlated to pharmaceutical concentrations in the Pearl River (China). For example, Regions 1, 2, and 4 were positively correlated to caffeine concentration $(R^2 = 0.86)$, but the humic and fulvic acid-like fluorescence (Region 3) and 5) were not associated with caffeine. Nevertheless, EEM regions are generally defined, and the observed fluorescence peaks often occur at different wavelengths (within the region) or cross the regional boundaries, potentially resulting in non-linear relationships with FDOM concentration.

To improve the specificity of fluorescence quantitation in EEMs, parallel factor analysis (PARAFAC) has been increasingly employed to identify independent components that can be used to reconstruct the observed fluorescence signals of real samples (Murphy et al., 2013). Chen et al. (2017) studied the influence of paved overflow and sanitary sewers on FDOM characterization during rain events and identified tryptophan- and tyrosine-like EEM-PARAFAC components as wastewater markers. Sgroi et al. (2017) found that maximum intensities of humic acid- and tyrosine-like fluorescence components were well correlated with other wastewater indicators (e.g., chemical oxygen demand, caffeine, ibuprofen) in two rivers that receive wastewater effluent. The aforementioned studies have focused on river networks (>seventh order streams) impacted by wastewater effluent; nevertheless, low-order urban streams warrant more attention due to their proximity and, therefore, vulnerability to failing sewer infrastructure. Specific fluorescence signals have only recently been explored as indicators of SSOs and sewer exfiltration in urban streams that do not receive wastewater effluent (Mendoza et al., 2020; Mladenov et al., 2022). No studies have been reported in urban watersheds with septic systems.

The specific objectives of this study were as follows: (1) to develop novel EEM-based parameters to identify the presence of wastewaterderived FDOM in urban streams; (2) to generate an EEM-PARAFAC model to improve the sensitivity and selectivity of fluorescence parameters as wastewater indicators; and (3) to compare spatiotemporal patterns in FDOM composition with CEC concentrations to confirm the presence of wastewater and validate the proposed fluorescence indicators. Importantly, EEM spectroscopy only requires 4-mL sample volumes, 10-min analysis times, and no major consumable costs. For these reasons, FDOM-based parameters were pursued as quick, easy, and cost-effective wastewater indicators compared to CECs. To address the objectives, monthly samples were collected from 27 sites in two urban watersheds over a one-year period. This large, spatially- and temporallyresolved FDOM dataset will not only address important knowledge gaps about the introduction of raw wastewater into urban streams from failing sewer infrastructure, but also provide key insights to FDOM composition in low-order urban streams.

2. Materials and methods

2.1. Chemicals and reagents

Suwannee River Natural Organic Matter (SRNOM) was purchased from the International Humic Substances Society (Denver, USA), and a 400 $\rm mg_{\rm C}~L^{-1}$ stock solution was prepared by reconstituting the freezedried isolate with deionized water following protocols similar to those reported by Apell et al. (2019). Then, the stock solution was diluted with deionized water to 4 $\rm mg_{\rm C}~L^{-1}$ and used (i) as a natural organic matter reference and (ii) for quality control purposes during EEM analysis. Oasis hydrophilic-lipophilic balanced cartridges (150 mg, 6 cm 3) were acquired from Waters Corp. (Milford, USA) for solid-phase extraction of CECs in water samples. LC-MS grade water, methanol, and acetonitrile were procured from Fisher Scientific (Hampton, USA) for analysis of 66 CECs by liquid chromatography with tandem mass spectrometry (LC-MS/MS). Additional details on the CECs, which included 43 antibiotics, 9 hormones, 13 UV filters, and 1 artificial sweetener, are available in Text S1 and Table S1.

2.2. Site information

The Baltimore sewer system was first constructed in 1915 and placed along stream valleys, including those of the Jones Falls and Gwynns Falls watersheds in Maryland, USA (Baltimore City, 2018b). Due to its age and poor maintenance, the 5000-km system suffers from regular SSOs and leaks (Baltimore City, 2018b, 2020; Baltimore County, 2020b). From April 2019 to March 2020, monthly water samples were collected from 27 locations in the Jones Falls (13 sites) and Gwynns Falls (14 sites) watersheds. These locations included 21 sites in first-, second-, or third-order (i.e., low-order) streams and 6 sites in medium-sized, fourth-order streams (Strahler, 1957). Raw wastewater samples were also collected from the sanitary sewer system at one site in the middle of the Gwynns Falls watershed (GWN-WW1), one site in the middle of the Jones Falls watershed (JON-WW1), and one site near the mouth of the Jones Falls (JON-WW2). Daily discharge data were obtained from two United States Geological Survey (USGS) flow gauges located in the Jones Falls (USGS 01589440) and Gwynns Falls (USGS 01589352). The sampling sites, wastewater collection locations, and USGS flow gauges are shown in Fig. 1. Detailed descriptions of land use, population, stream order, and other site-specific information are available in Text S2 and Table S2.

2.3. Sample collection

Monthly water samples were collected by partners at Blue Water Baltimore, placed on ice in a cooler for transport to the laboratory, and subsequently analyzed for FDOM (April 2019 to March 2020) and CECs

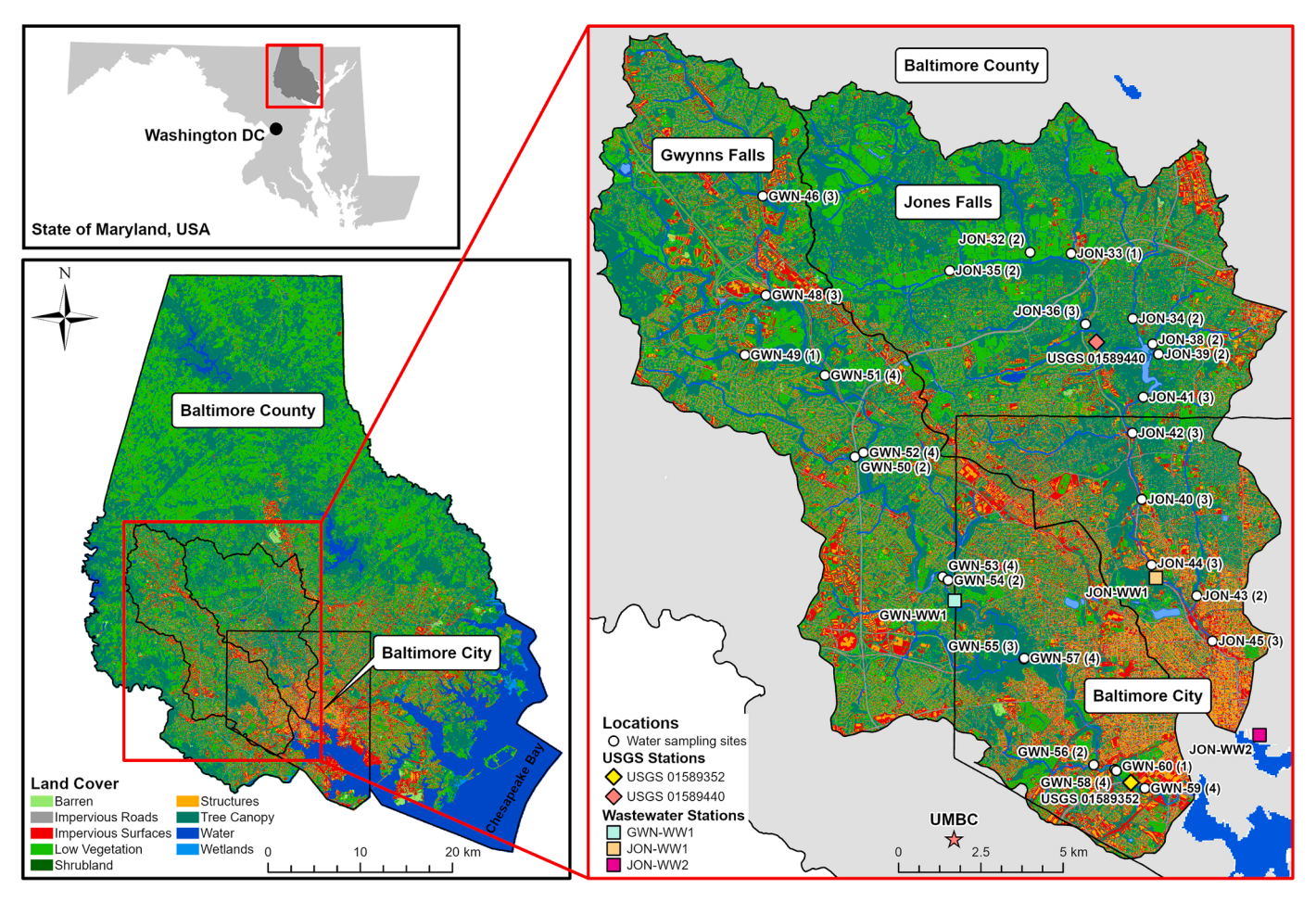


Fig. 1. Sampling locations in the Gwynns Falls and Jones Falls watersheds of Baltimore, Maryland, USA. The number in parentheses after each site code is the stream order. Land cover data were obtained from the Conservation Innovation Center Land Cover Data Project (https://www.chesapeakeconservancy.org).

(August 2019 to February/March 2020). For FDOM analysis, 100-mL samples were added to amber-glass containers and frozen at −20 °C until sample preprocessing for EEM analysis. A total of 296 water samples were analyzed during the 12-month sampling campaign; note, another 28 samples were either lost during transport/storage (i.e., broken bottles) or not collected due to weather conditions. No appreciable fluorescence was measured in the laboratory/field blanks. Based on the first four months of FDOM results, four sites were selected for monthly analysis of 66 CECs. The sites were chosen to examine CEC concentrations in urban (i.e., GWN-60, JON-45) and suburban/rural (i. e., GWN-55, JON-33) locations of each watershed. Samples were collected by submerging 1-L amber-glass bottles just below the water surface. A total of 16 wastewater samples were collected to enable FDOM and CEC comparisons between stream samples and raw wastewater from the same watershed. The samples were kept at 4 °C until sample preprocessing for LC-MS/MS analysis.

During sample collection, the dissolved oxygen, pH, specific conductance, and temperature were recorded using a multimeter YSI Pro-Plus Quatro (YSI Incorporated; Yellow Spring, USA). An AquaFluor fluorometer (Turner Design; San Jose, USA) was used to measure turbidity and the concentration of optical brighteners (wastewater indicators). A parallel set of water samples were collected for analysis of *Enterococcus* spp., total nitrogen, and total phosphorus. These data were obtained from a publicly-available database (Blue Water Baltimore, 2022).

2.4. Analysis of fluorescence EEMs

The water samples were thawed to room temperature, a 10-mL aliquot was passed through a 0.45-µm glass-fiber syringe filter, and the filtrate was added to a quartz cuvette with a 1-cm pathlength. Fluorescence EEMs were recorded for the filtered water samples using an Aqualog fluorometer (Horiba Scientific; Edison, USA). The excitation and emission wavelength ranges were 230-500 and 250-600 nm, respectively. To ensure highly resolved data, the excitation and emission wavelengths were incremented by 3.0 nm and 3.2 nm, respectively. The integration time was set to 2 s to ensure sensitivity and avoid photobleaching. A sealed Raman water fluorescence standard (Agilent Technologies; Santa Clara, USA) was used to convert all data to Raman Units (RU). The 1st and 2nd order Rayleigh scattering lines were removed by the Horiba masking tool. The fluorescence spectrum of deionized water was subtracted from the spectra of environmental samples to minimize the background response. Wastewater samples were diluted two times with deionized water to decrease inner-filter effects. SRNOM was analyzed between every six environmental samples for quality control purposes. The corrected EEM spectra were plotted and integrated in Matlab R2018b (Mathworks; Natick, USA). Due to the low CEC concentrations, fluorescence EEMs were solely attributed to FDOM.

The regional volumes (Φ_i) for each EEM were calculated using Eq. (1) (Chen et al., 2003). To improve the resolution of FDOM in Regions 1–4 relative to Region 5, the regional volumes were normalized to (i) the total volume under each EEM to obtain "fractional" volumes $(\Phi_{frac,i}; Eq. (2))$, (ii) the regional area to calculate "area-normalized" volumes $(\Phi_{area-norm,i}; Eq. (3))$, and (iii) the total volume of the area-normalized

EEMs to identify "fractional area-normalized" volumes ($\Phi_{frac,area-norm,i}$; Eq. (4)).

$$\Phi_{i} = \underset{ex(i)em(i)}{\sum} I_{FL}(\lambda_{ex}, \lambda_{em}) \Delta \lambda_{ex} \Delta \lambda_{em} \tag{1}$$

$$\Phi_{\text{frac},i} = \frac{\Phi_{i}}{\sum_{i} \Phi_{i}} \tag{2}$$

$$\Phi_{area-norm,i} = \frac{\sum_{ex(i)} \sum_{em(i)} I_{FL}(\lambda_{ex}, \lambda_{em}) \Delta \lambda_{ex} \Delta \lambda_{em}}{\Delta \lambda_{ex(i)} \Delta \lambda_{em(i)}} \tag{3}$$

$$\Phi_{\text{frac,area-norm,i}} = \frac{\Phi_{\text{area-norm,i}}}{\sum_{i} \Phi_{\text{area-norm,i}}}$$
(4)

In Eqs. (1)-(4), $I_{FL}(\lambda_{ex},\lambda_{em})$ is the fluorescence intensity at a particular excitation wavelength (λ_{ex}) and emission wavelength (λ_{em}), the summation terms (i.e., $\sum_{ex(i)}$, $\sum_{em(i)}$) cover the boundaries of Region i, $\Delta\lambda_{ex}$ and

 $\Delta\lambda_{em}$ were 3.0 nm and 3.2 nm, respectively, $\Delta\lambda_{ex(i)}$ and $\Delta\lambda_{em(i)}$ are the range of excitation and emission wavelengths for Region i, respectively, and, $\sum\!\Phi_{area-norm,i}$ is the total volume under the area-normalized EEM.

The calculated areas (*i.e.*, $\Delta \lambda_{ex(i)} \Delta \lambda_{em(i)}$) for Regions 1, 2, 3, 4, and 5 were 1600, 1000, 4400, 8450, and 47,800 nm², respectively, for the boundaries shown in Fig. S1.

Specific ratios of the fractional area-normalized volumes were calculated using Eqs. (5) and (6) to investigate their utility as wastewater indicators.

$$\frac{R4}{R5} = \frac{\Phi_{frac,area-norm,4}}{\Phi_{frac,area-norm,5}} \tag{5}$$

$$\frac{R2}{R5} = \frac{\Phi_{\text{frac},\text{area-norm},2}}{\Phi_{\text{frac},\text{area-norm},5}} \tag{6}$$

2.5. EEM-PARAFAC model development

Data from 296 EEMs were used to develop and validate an EEM-PARAFAC model according to the protocols of Murphy et al. (2013) with the drEEM (version 0.2.0) and N-way (version 3.30) toolboxes in Matlab. Due to high signal-to-noise ratios, preprocessing corrections were made by removing data for excitation wavelengths lower than 250 nm (Text S3). More details on the development and validation of the four-component EEM-PARAFAC model are available in Text S3. In accordance with best practices (Murphy et al., 2013), the maximum intensity (F_{max}) of the four fluorescent components was used to explore spatiotemporal changes in FDOM composition.

2.6. CEC analysis

The 1-L samples were passed through a 0.45- μ m glass-fiber filter and acidified to pH 3.0 (or lower) with 3 M HCl. Solid-phase extraction of 43 antibiotics, 9 hormones, 13 UV filters, and sucralose was conducted according to previous protocols (He et al., 2019; Mitchelmore et al., 2019). The selected CECs and their corresponding isotopically labeled standards are listed in Table S1. Extracts were stored in amber vials at $-20~^{\circ}\text{C}$ until analysis by LC-MS/MS (He et al., 2019; Mitchelmore et al., 2019). Laboratory and field blanks were prepared and analyzed according to the same protocols, and no CECs were detected.

3. Results and discussion

3.1. New EEM parameters to resolve spatiotemporal changes in FDOM composition

Fig. 2 shows EEMs measured in samples from a representative site, JON-45, across the 12-month campaign; note, EEMs from the other 26 sampling sites are provided in Fig. S2. The FDOM concentration exhibited clear differences from month to month, with higher levels

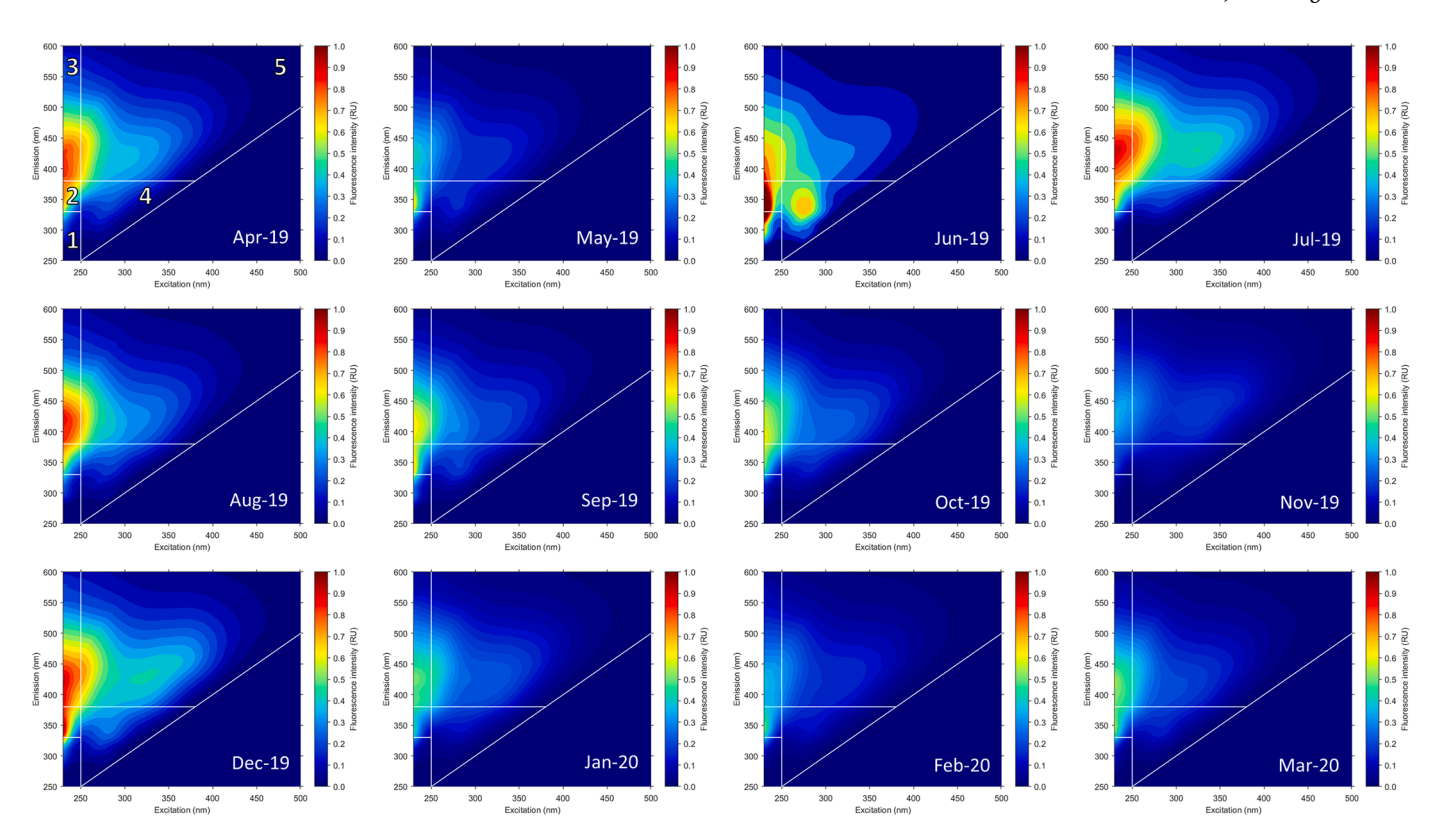


Fig. 2. EEMs measured in monthly samples from JON-45. White lines represent the boundaries of Regions 1, 2, 3, 4, and 5, which are defined in the April 2019 EEM (upper left corner). Note, EEMs for the other 26 sampling sites are available in Fig. S2.

present in April, June, July, August, and December. The fluorescence signatures, however, were similar for most months, with the exceptions of Regions 1, 2, and 4 for June. For example, the Region 4 volume for the June sample was 5007 RU nm 2 , 2.3× the average value from other months (2194 RU nm 2). The distributions of regional volumes calculated with Eq. (1) are presented in Fig. 3a.

The regional volumes in Fig. 3a are a function of FDOM concentration; therefore, these values were normalized to the total volume under each EEM using Eq. (2) to improve comparison of fluorescence responses in Regions 1–5. The "fractional" volume ($\Phi_{frac,i}$) distributions are reported in Fig. 3b. The humic acid-like fluorescence responses (Region 5) were dominant, accounting for 77.1 \pm 4.2% (average \pm standard deviation) of the total EEM volume across all samples. The fulvic acid-like (Region 3) and soluble microbial product-like (Region 4) fluorescence comprised 9.86 \pm 2.70% and 9.66 \pm 0.54% of the total fluorescence, respectively. The contributions of protein-like fluorescence were 2.43 \pm 0.71% (Region 2) and 0.98 \pm 0.59% (Region 1). The narrow interquartile ranges in Fig. 3b prevented clear interpretation of differences in Region 1–5 fluorescence between sampling sites and times. To improve comparison of regional differences, the "area-normalized" fluorescence $(\Phi_{\text{area-norm i}})$ volumes were calculated using Eq. (3). The corresponding distributions (Fig. 3c) showed a larger overlap between regions, indicating better spatiotemporal resolution.

Because the flow rate of each stream varied with time (Fig. S3), the

 Φ_i and $\Phi_{area-norm,i}$ fluorescence parameters, which are directly related to FDOM concentration, were naturally variable. For example, the areanormalized fluorescence $(\Phi_{area-norm,i})$ responses at GWN-58, which is in a fourth-order stream, were 0.13, 0.69, 0.62, 0.33, and 0.46 RU for Regions 1, 2, 3, 4, and 5, respectively, in September; however, these values increased to 0.23, 1.02, 0.81, 0.44, and 0.58 RU, respectively, in December. Because the responses were linearly correlated to each other (R² = 0.97), the observed differences were attributed to changes in FDOM concentration and not FDOM composition. The 24-h geometric mean discharges measured at USGS station 01589352, which is adjacent to GWN-58, were 0.524 and 3.115 m³ s $^{-1}$ in September and December (Table S3), respectively. Given the change in fluorescence magnitude (35% increase) and flow rate (495% increase), the increased discharge mobilized more FDOM into the stream but did not introduce new sources of FDOM.

Different trends were observed at other sites. For example, the June sample from JON-36, which is in a third-order stream, exhibited areanormalized fluorescence of 0.44, 1.08, 0.59, 0.53, and 0.32 RU for Regions 1, 2, 3, 4, and 5, respectively, but the fluorescence decreased to 0.02, 0.25, 0.25, 0.09, and 0.21 RU, respectively, in July. Unlike GWN-58, these fluorescence responses were not linearly correlated ($R^2 = 0.21$). The Jones Falls flow rate was measured at USGS station 01589440 in June (0.953 m³ s⁻¹) and July (1.744 m³ s⁻¹). The change in flow rate (83% increase) was driven by rain events (Fig. S3); however, the dilution

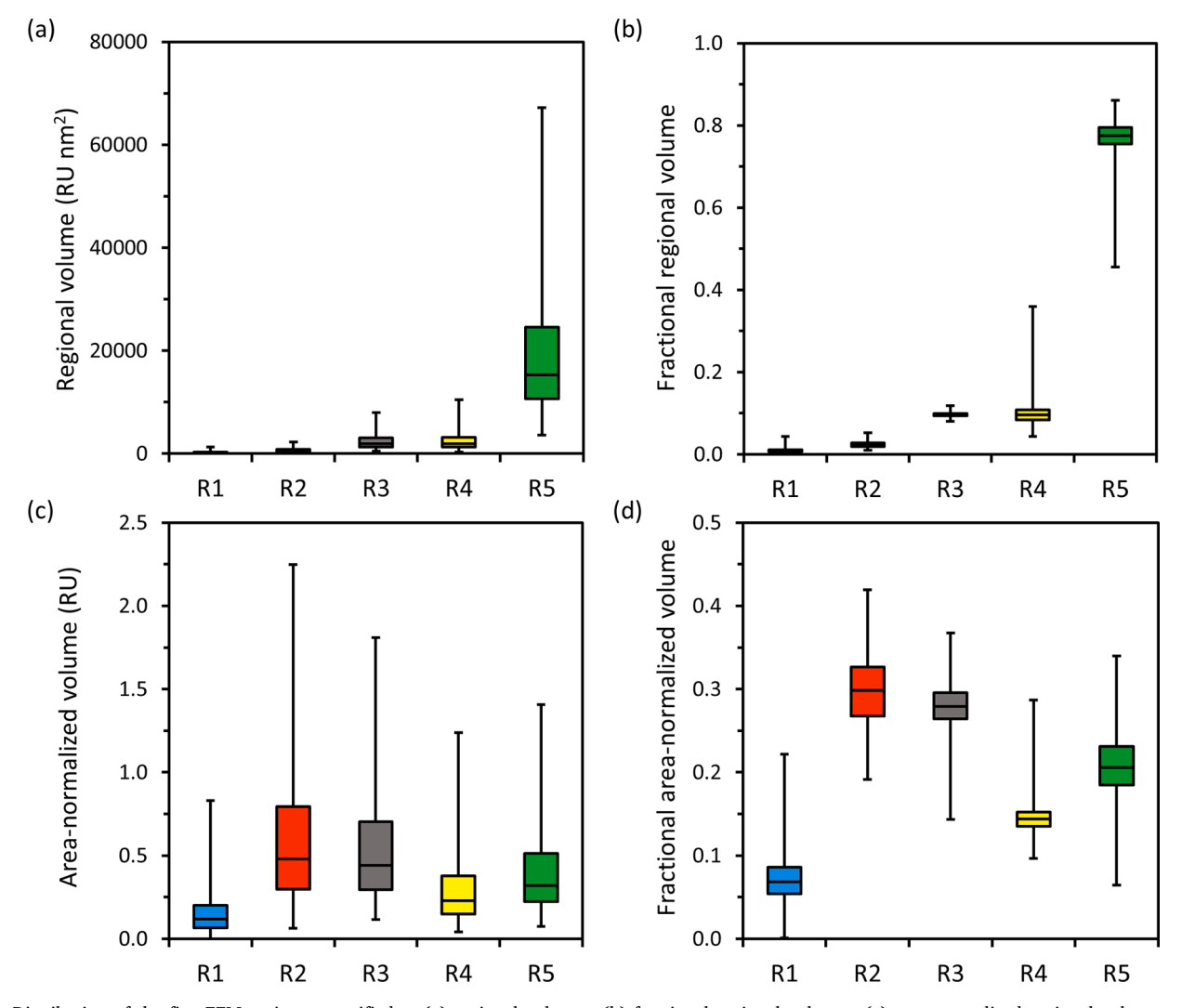


Fig. 3. Distribution of the five EEM regions quantified as (a) regional volumes, (b) fractional regional volumes, (c) area-normalized regional volumes, and (d) fractional, area-normalized regional volumes (n = 296).

factor could not fully account for the change in FDOM composition, suggesting inputs from other DOM sources in June.

To decouple FDOM concentration and composition, the fractional area-normalized volumes ($\Phi_{frac,area-norm,i}$, Eq. (4)) were calculated; the corresponding distributions are plotted in Fig. 3d. Regions 1, 2, 3, 4, and 5 comprised 7.3 \pm 3.1%, 29.8 \pm 4.1%, 27.8 \pm 2.9%, 14.4 \pm 1.7%, and 20.7 \pm 4.0% of the total area-normalized fluorescence volume, respectively. The more even distribution of regional fluorescence enabled better identification of differences in FDOM composition between samples.

3.2. Application of new EEM parameters to assess FDOM in urban streams

An initial analysis of the 296 EEMs highlighted a prominent and unique fluorescence response in Region 4 for 42 samples (e.g., JON-45 in June, Fig. 2). The raw wastewater samples also showed a strong fluorescence response in Region 4 (Fig. S4). To determine the relative presence of wastewater-derived FDOM against that of natural organic matter, the fractional area-normalized fluorescence volume of Region 4 was divided by the corresponding value for Region 5, and the resulting parameter was designated R4/R5 (Eq. (5)). Region 5 was employed in this ratiometric parameter due to the consistent fluorescence response of humic acid-like molecules in all samples. After evaluating the inflection point of the cumulative distribution of R4/R5, the top 20th percentile (i. e., R4/R5 = 0.85) was selected as a threshold to designate samples that are potentially influenced by wastewater (Fig. S5a). The 64 samples with R4/R5 greater than 0.85 included the 42 samples identified through initial EEM analysis. For example, R4/R5 was 1.30 for the June sample from JON-45. Although a prominent Region 4 response was not initially noted at JON-45 for the May sample due to the low FDOM concentration, the R4/R5 ratio was 0.88, highlighting a key advantage of the proposed ratiometric parameter.

Other ratios of fractional, area-normalized fluorescence volumes were also considered. In particular, R2/R5 (Eq. (6)) demonstrated potential for identification of wastewater inputs, as evidenced by the raw wastewater EEM in Fig. S4, which exhibited notable fluorescence intensity in Region 2. The cumulative distribution of R2/R5 (Fig. S5b) was used to determine a threshold at the top 20^{th} percentile (i.e., R2/R5 = 1.85). Using the R2/R5 parameter, 60 samples were identified as being potentially impacted by wastewater, including JON-45 in May (R2/R5 = 2.30) and June (3.14). In total, 46 samples exhibited high R4/R5 and R2/R5.

Previous reports have also used the ratio of fluorescence responses to screen for changes in FDOM composition and water quality; however, those efforts employed the ratios of peak intensities at specific, preselected excitation/emission wavelengths ($\lambda_{ex/em}$). For example, Baker (2001) proposed the ratio of tryptophan-like ($\lambda_{ex/em} = 275/350$ nm) to fulvic acid-like ($\lambda_{ex/em} = 320-340/410-430$ nm) fluorescence peaks to identify wastewater effluent in rivers. Similarly, Mendoza et al. (2020) developed a fluorescence sensor that employed the tryptophan-like ($\lambda_{ex/em} = 280/340$ nm) to humic acid-like ($\lambda_{ex/em} = 325/470$ nm) ratio to detect untreated wastewater inputs in urban streams during storm events. The proposed R2/R5 parameter is functionally similar to the above approach but serves as a more robust indicator due to the use of wider excitation and emission ranges, which are less likely to be influenced by local variability in measured EEMs.

The proposed fluorescence indicators were contextualized by analyzing SRNOM and raw wastewater (Fig. S4). The R4/R5 ratios measured in SRNOM and raw wastewater were 0.22 ± 0.05 (n=20) and 1.64 ± 0.25 (n=16), respectively; similarly, the R2/R5 ratios were 0.38 ± 0.05 (n=20) and 4.13 ± 0.35 (n=16), respectively. Clearly, the SRNOM exhibited low R4/R5 and R2/R5, and the raw wastewater exceeded the proposed thresholds (Fig. S6). These results support the utility of the R4/R5 and R2/R5 parameters as "first-pass" indicators of wastewater in low- and medium-order streams. Nevertheless, the

observed fluorescence peaks in Regions 2, 4, and 5 often cross the regional boundaries (Fig. S1), which may affect the accuracy of EEM-based parameters. To improve the specificity of fluorescence-based wastewater indicators, an EEM-PARAFAC model was developed to deconvolute the data into distinct fluorescence components.

3.3. EEM-PARAFAC model

More details about the preliminary EEM-PARAFAC models are available in Text S3, Table S4, and Fig. S7. The three- and fivecomponent EEM-PARAFAC models exhibited a higher sum of the squared errors and a lower core consistency than the four-component model, respectively; furthermore, the six-, seven-, and eightcomponent models contained unrealistic spectral features. The four components of the final, validated EEM-PARAFAC model are presented in Fig. 4a, and the corresponding excitation and emission loadings are provided in Fig. S8. Watershed-specific models were also evaluated and found to match the global model (Table S4). Component 1 (C1) had an excitation peak at 250 nm and an emission peak at 410 nm. With two excitation peaks at 262 and 355 nm, Component 2 (C2) primarily emitted at 455 nm. The excitation loading of Component 3 (C3) was similar to C2 with one peak at 262 nm, but the second peak shifted up to 394 nm; in addition, the wavelength of the emission peak increased to 495 nm. Component 4 (C4) displayed excitation and emission peaks at 274 nm and 335 nm, respectively. The fluorescence responses of C1, C2, and C3 were primarily located in Region 5 ($\Phi_{frac.5} > 0.98$ for all three components), but the fluorescence of C4 was split between Region 4 $(\Phi_{frac,4}=0.723)$ and Region 5 $(\Phi_{frac,5}=0.248)$. The co-occurrence of three unique components in Region 5 and the split-presence of another component between two regions reinforced concerns about the lack of specificity when using regional volumes for quantitative FDOM analysis. Importantly, the unique fluorescence spectra of C1, C2, and C3 suggest that these components stem from different sources and exhibit variable fate and transport in urban watersheds. Correlation analysis of component scores before (Fig. S9) and after (Fig. S10) data normalization confirmed the independent nature of the components. Due to its high excitation and emission wavelengths, C3 was comprised of more hydrophobic, high molecular weight compounds than C1 and C2 (Ishii and Boyer, 2012; Wu et al., 2003).

The excitation and emission loadings of C1, C2, C3, and C4 were uploaded to the OpenFluor database (Murphy et al., 2014) and generated matches (Tucker's correlation coefficient > 0.95) with previously reported spectra from 60, 10, 62, and 45 studies, respectively (as of July 2022). The top 10 matches for each component are shown in Table S5. For example, C1 was similar to a terrestrial humic-like component from the Neuse River estuary (USA) (Osburn et al., 2012), a microbial humic-like component from the Otonabee River (Canada) (Peleato et al., 2016), and a microbial humic-like component from the Nakdong River watershed (South Korea) (Derrien et al., 2019). C2 aligned with a humic-like component from Lake Lillsjön (Sweden) (Wünsch et al., 2017) and a terrestrial humic-like component in the Meuse River (Belgium) (Lambert et al., 2017). With the highest number of matches, C3 exhibited spectral similarities to terrestrial fulvic-like components reported for water bodies in Quebec (Canada) (Lapierre and del Giorgio, 2014), soil extracts from a forested watershed in Costa Rica (Osburn et al., 2018), and water from the Arno River (Italy) (Retelletti Brogi et al., 2020). C4 was similar to tryptophan-like fluorescence components reported in studies that involved biological wastewater treatment processes (Jia et al., 2017; Murphy et al., 2011) or wastewater-impacted rivers (Retelletti Brogi et al., 2019; Yu et al., 2015); however, this component was also related to decomposition of aquatic plants in China (Yuan et al., 2020), highlighting the importance of developing EEM-PARAFAC models at the watershed scale. The primary associations of C1, C2, and C3 with natural DOM and C4 with wastewater confirmed the potential for C4 to be used as a wastewater indicator.

The distributions of F_{max} values for each component are presented in

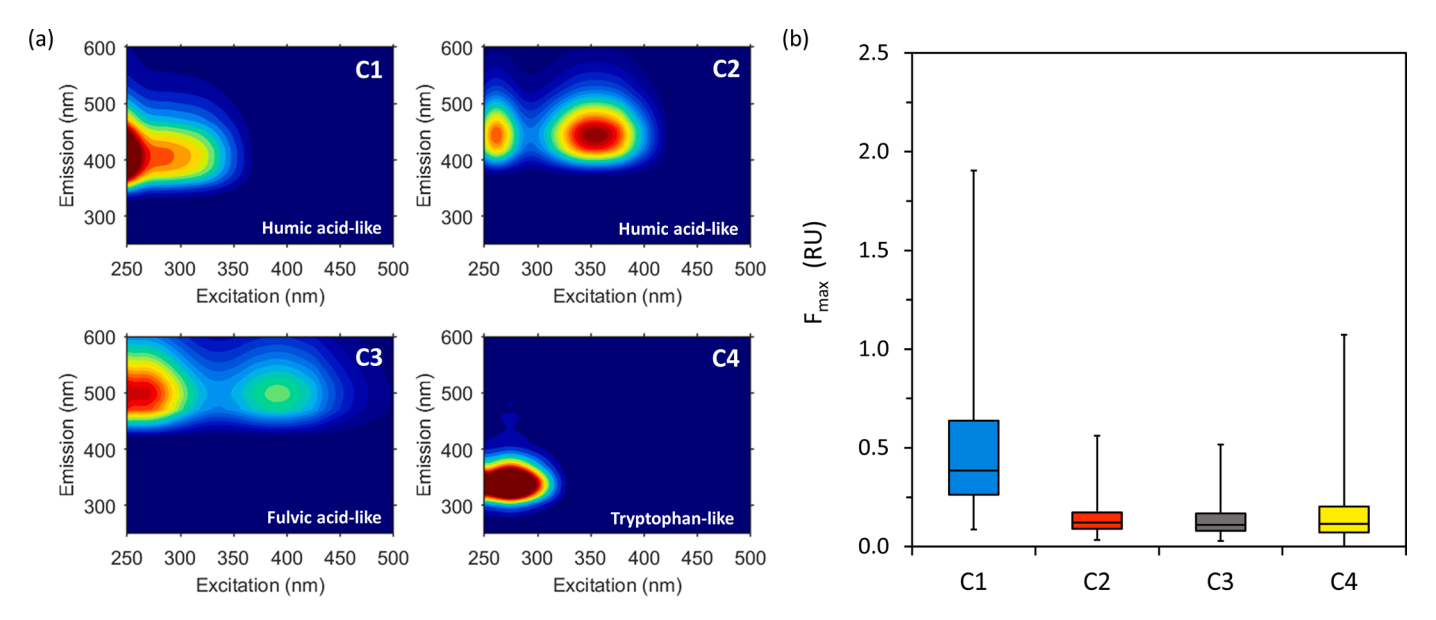


Fig. 4. The (a) fluorescence signatures of the four EEM-PARAFAC model components and (b) F_{max} distributions for each component across all samples (n = 295). The excitation and emission loadings are available in Fig. S8.

Fig. 4b, and the F_{max} values are plotted for each site in Fig. S11. As indicated above, tryptophan-like fluorescence has been associated with wastewater-impacted groundwater (Lapworth et al., 2008; Lee et al., 2015) and surface water (Baker 2001; Baker and Inverarity 2004). The F_{max} values of C4 in some samples (e.g., GWN-60 in June; JON-33 in July and December; and, JON-45 in June) were obviously greater than at other sites and times. For example, the F_{max} values of C4 at JON-45 and GWN-60 in June were about $4\times$ the average of the other samples, suggesting unique sources of this fluorescence component in those samples.

3.4. Ratiometric EEM-PARAFAC indicators and their spatiotemporal trends

To account for differences in FDOM concentration, the ratios of C4 with the other components were evaluated. The cumulative distributions of the C4/C1, C4/C2, and C4/C3 ratios were assembled (Fig. S12) and used to identify thresholds at the top 20^{th} percentiles, namely 0.37, 1.35, and 1.45, respectively. The wider range and higher threshold of the C4/C3 parameter provided more resolution and better specificity. According to the C4/C3 threshold, 29 samples from the Jones Falls and 30 samples from the Gwynns Falls were potentially impacted by wastewater. Importantly, the R4/R5 and C4/C3 parameters were well correlated (R² = 0.88; Fig. S13). While both metrics suggested wastewater influence, the slope of C4/C3 vs. R4/R5 (4.14) was greater than 1.0, confirming the better sensitivity of the C4/C3 parameter.

The spatiotemporal trends of C4/C3 and R4/R5 are presented for both watersheds in Fig. 5. In the Jones Falls watershed, 20 of the samples with C4/C3 greater than 1.45 were located in the more rural/suburban upper stretch (i.e., JON-32 to JON-39), and the other nine were in the more urban lower section (i.e., JON-40 to JON-45). The upstream sites were generally in first- and second-order streams situated in areas with less sewers and more septic systems. In fact, the Jones Falls watershed has 3244 septic systems (Topolski 2021), and they are primarily located in the upstream area (Fig. S14). Previous literature has confirmed that septic systems (i) increase nutrient inputs and contribute to eutrophication in rural headwaters (Withers et al., 2011; Withers et al., 2012), (ii) introduce CECs into rural streams (Ramage et al., 2019; Spoelstra et al., 2020), and (iii) impact water quality in other regional watersheds (Harrison et al., 2012; Reay 2004; Shields et al., 2008). The prevalence of the high C4/C3 signals in the upstream locations may, therefore, stem from septic system discharges. The Jones Falls watershed has $3.5 \times$ more septic systems than the Gwynns Falls watershed (Topolski, 2021), which did not exhibit high C4/C3 at the upstream locations. While 21/29 samples with high C4/C3 were recorded in the spring and early summer months (*i.e.*, April, May, June, July), only eight samples demonstrated high C4/C3 in the late summer, fall, and winter (*i.e.*, August 2019 to March 2020). These results suggested the potential influence of seasonal precipitation and/or stream flow rate on the C4/C3 parameter.

To further investigate this phenomenon, the 24-h geometric average discharge (prior to sample collection) was calculated using data obtained from USGS flow gauges located near JON-36 and GWN-58 (Table S3). The C4/C3 ratios were plotted against stream flow rate in Fig. S15. For JON-36, the April, June, and January samples demonstrated high C4/C3, but no discernable trends were observed with flow rate. At GWN-58, 8/9 samples exhibited C4/C3 values lower than the threshold. The April sample had a high C4/C3, but the flow rate (2.057 $\rm m^3~s^{-1})$) was in the middle of the range (0.524–3.115 $\rm m^3~s^{-1})$). Accordingly, no influence of volumetric flow rate was noted with respect to the C4/C3 parameter.

In the Gwynns Falls watershed, 30 samples exhibited high C4/C3, with clear evidence of hotspots at GWN-53 (4/12 months), GWN-54 (5/ 12 months), and GWN-60 (10/11 months). These three sites are fourth-, second, and first-order streams located in a high-density urban section of Baltimore City where SSOs have been frequently reported (Baltimore County, 2020a; Lien et al., 2005). In fact, the average Enterococcus spp. count at these three sites was 1600 most probable number (MPN)/100 mL (Blue Water Baltimore, 2022), 11× higher than the human health threshold for body-contact water recreation (Maryland, 2022), supporting the relationship between high C4/C3 ratios and wastewater content. The four GWN-53 samples with high C4/C3 were collected in spring and early summer (i.e., April–July); however, no obvious temporal patterns were ascertained for C4/C3 at GWN-54, where the highest values were recorded in August and November. At GWN-60, the January sample was the only one that did not exceed the C4/C3 threshold. The consistently high C4/C3 ratios at GWN-54 and GWN-60 suggested continuous inputs from sewer exfiltration or SSOs in these low-order streams.

3.5. Occurrence of CECs and water quality indicators at sites of interest

Four of the 27 sites were selected for monthly analysis of 66 CECs in urban (i.e., GWN-60, JON-45) and suburban/rural (i.e., GWN-55, JON-

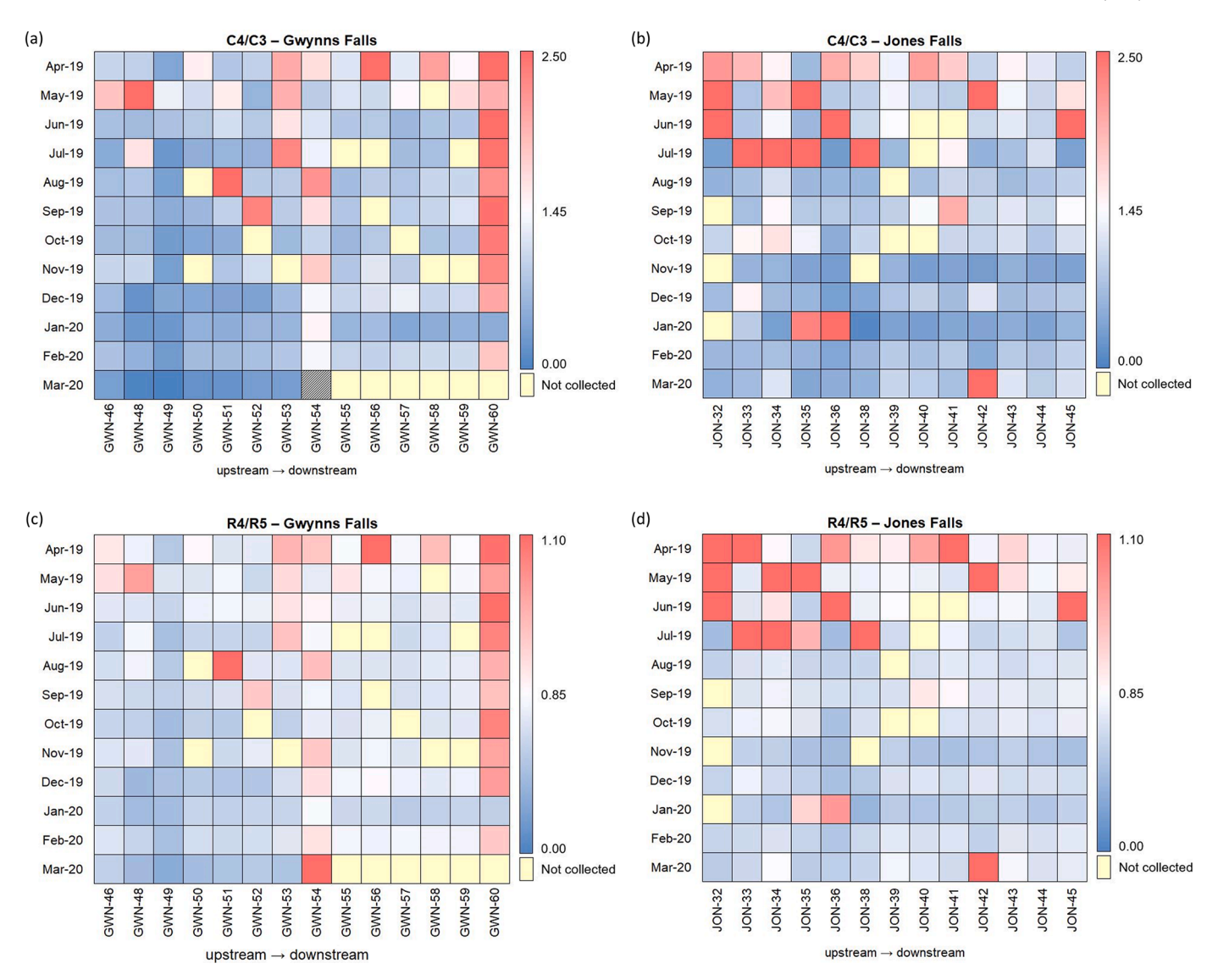


Fig. 5. Spatiotemporal trends for the (a,b) C4/C3 and (c,d) R4/R5 ratios in the (a,c) Gwynns Falls and (b,d) Jones Falls watersheds. The white color is associated with the threshold values (i.e., C4/C3 = 1.45, R4/R5 = 0.85), and the red and blue colors indicate higher and lower values, respectively. Note, the March sample from GWN-54 was confirmed as an outlier by the EEM-PARAFAC model (Text S3); therefore, C4/C3 was not reported for this sample.

33) locations of each watershed. Of the measured CECs, the artificial sweetener sucralose, which is regularly used as an indicator of wastewater effluent (Ramage et al., 2019; Spoelstra et al., 2020), was detected most frequently (19/28 samples) and at concentrations of 207-1354 ng L^{-1} (Fig. 6). In fact, sucralose was present in every sample from the urban GWN-60 site. Two UV filters, octocrylene (up to 141 ng L⁻¹) and oxybenzone (up to 212 ng L^{-1}), and the antibiotic sulfamethoxazole (up to 42 ng L⁻¹) were also detected at GWN-60. Illicit drugs (Lee et al., 2016) and pharmaceuticals (Fork et al., 2021) have been previously reported in the Gwynns Falls; furthermore, UV filters and estrogenic hormones were found to accumulate in crayfish from this watershed (He al., 2017). These findings reinforced the presence of anthropogenically-derived compounds in this first-order stream that does not receive wastewater effluent. Importantly, GWN-60 exceeded the C4/C3 and R4/R5 thresholds in 10/11 months (Fig. 5), supporting the application of ratiometric EEM-PARAFAC parameters as wastewater indicators.

The maximum sucralose concentration (1354 ng L^{-1}) was measured at GWN-55; furthermore, sulfamethoxazole (up to 108 ng L^{-1}), octocrylene (up to 148 ng L^{-1}), and oxybenzone (up to 192 ng L^{-1}) were also detected at this site (Fig. 6). The average *Enterococcus* spp. counts at

GWN-55 (824 MPN/100 mL) (Blue Water Baltimore, 2022) were $2.5-5.3\times$ higher than the average for the upper Gwynns Falls and the bacterial threshold for Maryland recreational waters (Maryland, 2022). However, the EEM-PARAFAC parameters at GWN-55 were below the identified thresholds. Similar results were reported in a previous study, in which sucralose and sulfamethoxazole concentrations did not correlate to a tryptophan-like wastewater indicator in specific locations (Sgroi et al., 2017).

The contrasting conclusions from the CEC concentrations, bacteria levels, and EEM-PARAFAC parameters at GWN-55 were considered according to (i) the locations of potential wastewater sources in upstream areas, (ii) the hydrological and land cover features in the sampling area, and (iii) the persistence of the CEC and EEM-PARAFAC indicators. The area immediately adjacent to GWN-55 contained the highest percentage of tree canopy and vegetation for the Gwynns Falls watershed (Fig. S16), but this site was also located downstream of the highly urbanized Dead Run subwatershed. The presence of sucralose and sulfamethoxazole at GWN-55 suggested that wastewater inputs occur upstream and undergo transport to downstream locations. These two CECs are conservative wastewater indicators that persist in surface water (McCance et al., 2018; Oppenheimer et al., 2011). In contrast, tryptophan-like FDOM

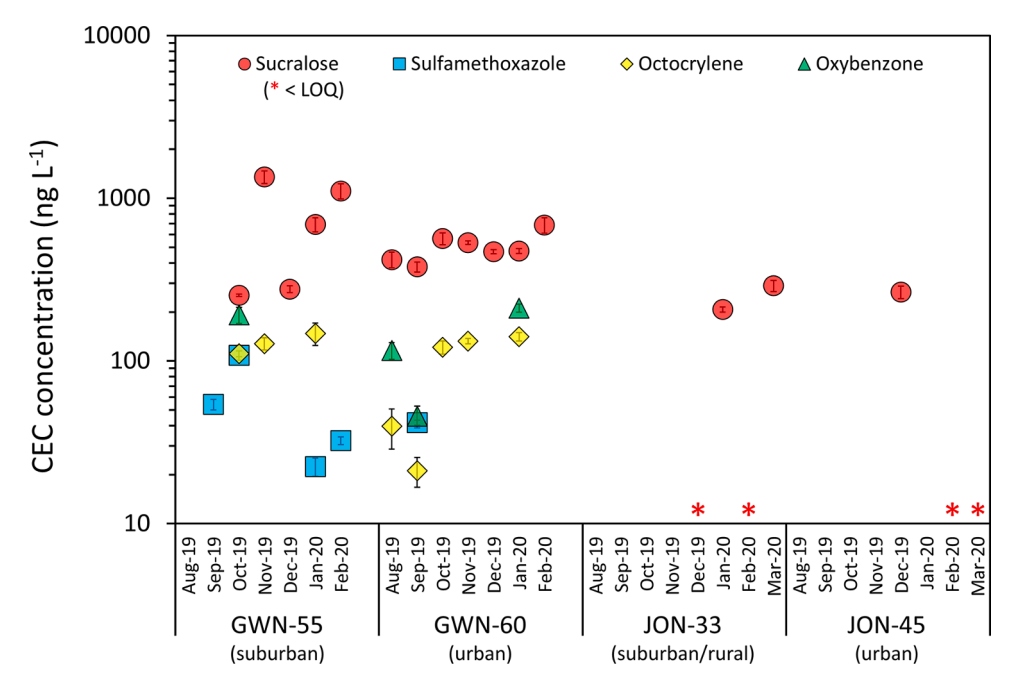


Fig. 6. CEC concentrations detected in the urban and suburban/rural sampling sites of the Jones Falls and Gwynns Falls. CECs are only shown if they were detected above their corresponding limit of detection; the "< LOQ" notation means below the limit of quantitation. Error bars are standard deviation (n = 3).

(C4) is more labile (Baghoth et al., 2011; Huang et al., 2015), which may explain the low C4/C3 ratios relative to the high sucralose and sulfamethoxazole contents. The other sites with high EEM-PARAFAC ratios were located in first- and second-order streams, but GWN-55 is in a third-order stream with further transport distances from primary wastewater sources. These data suggest that the EEM-PARAFAC parameters are sensitive indicators of nearby wastewater sources, providing more specific information about the locations of failing sewer infrastructure.

The detection frequency and concentrations of sucralose in the Jones Falls were lower than in the Gwynns Falls. At the JON-33 site, sucralose was detected in 4/7 samples at concentrations as high as 290 ng L⁻¹. These findings were somewhat surprising because JON-33 is located in a rural/suburban section of the upper Jones Falls, but the presence of sucralose at this site bolstered the conclusions developed from the C4/ C3 data, namely that septic systems (Fig. S14) serve as an important source of wastewater-derived chemicals. This conclusion was also supported by a report from a rural area in Canada, where septic systems were the main source of sucralose in streams that do not receive municipal wastewater effluent (Spoelstra et al., 2020). Sucralose was also detected in 3/7 samples from the urban JON-45 site at concentrations up to 265 ng L^{-1} , with wastewater exfiltration and SSOs being likely sources based on known occurrences in this area (Baltimore City, 2018a; Dance, 2017; Wells, 2015). High C4/C3 values and Enterococcus spp. counts (Blue Water Baltimore, 2022) were also recorded at JON-45, providing convincing evidence of sewer leaks at this site.

4. Conclusions

- We used novel EEM and EEM-PARAFAC parameters to distinguish between natural and wastewater-derived FDOM in low-order, urban streams that do not receive wastewater effluent but are impacted by SSOs, sewer exfiltration, and septic systems.
- The specific thresholds for the proposed EEM-PARAFAC ratios (C4/ C3 \geq 1.45 and R4/R5 \geq 0.85) were evaluated using a large dataset of 296 samples collected from 27 sites over a one-year period in two watersheds with variable land use. The proposed ratiometric parameters directly informed FDOM composition and were robust with respect to dilution effects caused by precipitation.

- Given the aging infrastructure and under-resourced maintenance of sewer systems in locations around the world, the R4/R5 parameter represents a quick, easy, and scalable "first-pass" technique to investigate the presence of wastewater in streams. For long-term monitoring and evaluation of water quality in the sampled watersheds, C4/C3 represents a more sensitive option. While the specific FDOM signatures may vary in other urban watersheds, the reported approach will enable quick and economical screening for the presence of wastewater.
- The FDOM parameters, measured CEC concentrations, and bacterial indicators confirmed wastewater influences at JON-45, GWN-54, and GWN-60. At GWN-55, CEC concentrations (up to 1354 ng L⁻¹) suggested the presence of wastewater, but this conclusion did not match the low response of fluorescence indicators. This outcome was postulated to stem from the higher lability of FDOM, which allowed more specific identification of nearby wastewater sources. As a result, we hypothesized that the wastewater inputs in this tributary occurred further upstream. Future efforts are recommended to evaluate quantitative correlations between fluorescence parameters, CEC concentrations, and bacterial indicators to enable implementation of quick, easy, and cost-effective FDOM-based wastewater indicators in low- and medium-order urban streams.
- The FDOM analysis suggested wastewater was present in rural/suburban sections of the Jones Falls watershed (e.g., JON-32, JON-33, JON-35), an unexpected phenomenon due to the low population density and development. The presence of sucralose up to 290 ng L⁻¹ at these sites validated the FDOM results and provided important insight into the influence of septic systems on urban/suburban streams.

Declaration of Competing Interest

The authors declare that they have no known competing financial interests or personal relationships that could have appeared to influence the work reported in this paper.

Data availability

Data are available in the supporting information and can also be

provided upon request

Acknowledgments

This work was supported by the National Science Foundation (#1653726). We acknowledge the Fulbright foreign student program and National Secretary of Science and Technology (SENACYT) of Panama for the doctoral scholarship to J.A. Batista-Andrade. We also thank Blue Water Baltimore for assistance with sample collection.

Supplementary materials

Supplementary material associated with this article can be found, in the online version, at doi:10.1016/j.watres.2022.119521.

References

- Apell, J.N., Pflug, N.C., McNeill, K., 2019. Photodegradation of fludioxonil and other pyrroles: the importance of indirect photodegradation for understanding environmental fate and photoproduct formation. Environ. Sci. Technol. 53 (19), 11240–11250.
- Ashley, R.M., Fraser, A., Burrows, R., Blanksby, J., 2000. The management of sediment in combined sewers. Urban Water 2 (4), 263–275.
- Baghoth, S.A., Sharma, S.K., Amy, G.L., 2011. Tracking natural organic matter (NOM) in a drinking water treatment plant using fluorescence excitation–emission matrices and PARAFAC. Water Res. 45 (2), 797–809.
- Baker, A., 2001. Fluorescence excitation—emission matrix characterization of some sewage-impacted rivers. Environ. Sci. Technol. 35 (5), 948–953.
- Baker, A., Inverarity, R., 2004. Protein-like fluorescence intensity as a possible tool for determining river water quality. Hydrol. Process. 18 (15), 2927–2945.
- Baltimore City, 2018a. Department of Public Works, Heavy Labor Day Weekend Rain Leads to SSOs. Baltimore City Department of Public Works, Baltimore, MD.
- Baltimore City (2018b) Department of public works, history of the system.
 Baltimore City, 2020. Department of Public Works. Sanitary Sewer Overflow (SSO)
- Public Notices.
 Baltimore County, 2020a. Gwynns Falls Watershed. Baltimore County Government,
- Baltimore, MD USA. Sustainability, E.P.a. (ed).
- Baltimore County, 2020b. Master Plan 2020. Baltimore County Government, Baltimore, MD, USA.
- Barbosa, M.O., Ribeiro, A.R., Ratola, N., Hain, E., Homem, V., Pereira, M.F.R., Blaney, L., Silva, A.M.T., 2018. Spatial and seasonal occurrence of micropollutants in four Portuguese rivers and a case study for fluorescence excitation-emission matrices. Sci. Total Environ. 644, 1128–1140.
- Berendonk, T.U., Manaia, C.M., Merlin, C., Fatta-Kassinos, D., Cytryn, E., Walsh, F., Bürgmann, H., Sørum, H., Norström, M., Pons, M.-N., Kreuzinger, N., Huovinen, P., Stefani, S., Schwartz, T., Kisand, V., Baquero, F., Martinez, J.L., 2015. Tackling antibiotic resistance: the environmental framework. Nat. Rev. Microbiol. 13 (5), 310–317.
- Blue Water Baltimore (2022) Data available at: https://baltimorewaterwatch.org/down load-data, Baltimore, MD.
- Chen, H., Liao, Z.-l., Gu, X.-y., Xie, J.-q., Li, H.-z., Zhang, J., 2017. Anthropogenic influences of paved runoff and sanitary sewage on the dissolved organic matter quality of wet weather overflows: an excitation–emission matrix parallel factor analysis assessment. Environ. Sci. Technol. 51 (3), 1157–1167.
- Chen, W., Westerhoff, P., Leenheer, J.A., Booksh, K., 2003. Fluorescence excitation—emission matrix regional integration to quantify spectra for dissolved organic matter. Environ. Sci. Technol. 37 (24), 5701–5710.
- Dance, S., 2017. Baltimore Sewer Pipe Was Sawed off, Connected to Storm Drain Leaking Into Jones Falls, Officials Say. The Baltimore Sun, Baltimore, MD.
- de Cock, M., van de Bor, M., 2014. Obesogenic effects of endocrine disruptors, what do we know from animal and human studies? Environ. Int. 70, 15–24.
- Derrien, M., Brogi, S.R., Gonçalves-Araujo, R., 2019. Characterization of aquatic organic matter: assessment, perspectives and research priorities. Water Res. 163, 114908.
- Durukan, S., Karadagli, F., 2019. Physical characteristics, fiber compositions, and tensile properties of nonwoven wipes and toilet papers in relevance to what is flushable. Sci. Total Environ. 697, 134135.
- Fork, M.L., Fick, J.B., Reisinger, A.J., Rosi, E.J., 2021. Dosing the coast: leaking sewage infrastructure delivers large annual doses and dynamic mixtures of pharmaceuticals to urban rivers. Environ. Sci. Technol. 55 (17), 11637–11645.
- Gonçalves-Araujo, R., Granskog, M.A., Bracher, A., Azetsu-Scott, K., Dodd, P.A., Stedmon, C.A., 2016. Using fluorescent dissolved organic matter to trace and distinguish the origin of Arctic surface waters. Sci. Rep. 6 (1), 33978.
- Guo, W., Xu, J., Wang, J., Wen, Y., Zhuo, J., Yan, Y., 2010. Characterization of dissolved organic matter in urban sewage using excitation emission matrix fluorescence spectroscopy and parallel factor analysis. J. Environ. Sci. 22 (11), 1728–1734.
- Harrison, M., Stanwyck, E., Beckingham, B., Starry, O., Hanlon, B., Newcomer, J., 2012. Smart growth and the septic tank: wastewater treatment and growth management in the Baltimore region. Land Use Policy 29 (3), 483–492.

He, K., Hain, E., Timm, A., Tarnowski, M., Blaney, L., 2019. Occurrence of antibiotics, estrogenic hormones, and UV-filters in water, sediment, and oyster tissue from the Chesapeake Bay. Sci. Total Environ. 650, 3101–3109.

- He, K., Timm, A., Blaney, L., 2017. Simultaneous determination of UV-filters and estrogens in aquatic invertebrates by modified quick, easy, cheap, effective, rugged, and safe extraction and liquid chromatography tandem mass spectrometry. J. Chromatogr. A 1509, 91–101.
- Huang, S.-b., Wang, Y.-x., Ma, T., Tong, L., Wang, Y.-y., Liu, C.-r., Zhao, L., 2015. Linking groundwater dissolved organic matter to sedimentary organic matter from a fluviolacustrine aquifer at Jianghan Plain, China by EEM-PARAFAC and hydrochemical analyses. Sci. Total Environ.t 529, 131–139.
- Hudson, N., Baker, A., Reynolds, D., 2007. Fluorescence analysis of dissolved organic matter in natural, waste and polluted waters—a review. River Res. Appl. 23 (6), 631–649.
- Ishii, S.K.L., Boyer, T.H., 2012. Behavior of reoccurring PARAFAC components in fluorescent dissolved organic matter in natural and engineered systems: a critical review. Environ. Sci. Technol. 46 (4), 2006–2017.
- Jagai, J.S., DeFlorio-Barker, S., Lin, C.J., Hilborn, E.D., Wade, T.J., 2017. Sanitary sewer overflows and emergency room visits for gastrointestinal illness: analysis of massachusetts data, 2006-2007. Environ. Health Perspect. 125 (11), 117007.
- Jia, F., Yang, Q., Liu, X., Li, X., Li, B., Zhang, L., Peng, Y., 2017. Stratification of extracellular polymeric substances (EPS) for aggregated anammox microorganisms. Environ. Sci. Technol. 51 (6), 3260–3268.
- Karpf, C., Krebs, P., 2011. Quantification of groundwater infiltration and surface water inflows in urban sewer networks based on a multiple model approach. Water Res. 45 (10), 3129–3136.
- Lambert, T., Bouillon, S., Darchambeau, F., Morana, C., Roland, F.A.E., Descy, J.-.P., Borges, A.V., 2017. Effects of human land use on the terrestrial and aquatic sources of fluvial organic matter in a temperate river basin (The Meuse River, Belgium). Biogeochemistry 136 (2), 191–211.
- Lapierre, J.F., del Giorgio, P.A., 2014. Partial coupling and differential regulation of biologically and photochemically labile dissolved organic carbon across boreal aquatic networks. Biogeosciences 11 (20), 5969–5985.
- Lapworth, D.J., Gooddy, D.C., Butcher, A.S., Morris, B.L., 2008. Tracing groundwater flow and sources of organic carbon in sandstone aquifers using fluorescence properties of dissolved organic matter (DOM). Appl. Geochem. 23 (12), 3384–3390.
- Lee, D.G., Roehrdanz, P.R., Feraud, M., Ervin, J., Anumol, T., Jia, A., Park, M., Tamez, C., Morelius, E.W., Gardea-Torresdey, J.L., Izbicki, J., Means, J.C., Snyder, S.A., Holden, P.A., 2015. Wastewater compounds in urban shallow groundwater wells correspond to exfiltration probabilities of nearby sewers. Water Res. 85, 467–475.
- Lee, S.S., Paspalof, A.M., Snow, D.D., Richmond, E.K., Rosi-Marshall, E.J., Kelly, J.J., 2016. Occurrence and potential biological effects of amphetamine on stream communities. Environ. Sci. Technol. 50 (17), 9727–9735.
- Lien, C., Brennan, K., Stewart, S. and Stack, B. (2005) Managing Watersheds for Human and Natural Impacts, pp. 1–9.
- Maryland, 2022. Department of the Environment, Water Quality Criteria Specific to Designated Uses. Maryland Department of the Environment, Annapolis, MD.
- McCance, W., Jones, O.A.H., Edwards, M., Surapaneni, A., Chadalavada, S., Currell, M., 2018. Contaminants of Emerging Concern as novel groundwater tracers for delineating wastewater impacts in urban and peri-urban areas. Water Res. 146, 118-133
- Mendoza, İ.M., Mladenov, N., Kinoshita, A.M., Pinongcos, F., Verbyla, M.E., Gersberg, R., 2020. Fluorescence-based monitoring of anthropogenic pollutant inputs to an urban stream in Southern California, USA. Sci. Total Environ. 718, 137206.
- Mitchelmore, C.L., He, K., Gonsior, M., Hain, E., Heyes, A., Clark, C., Younger, R., Schmitt-Kopplin, P., Feerick, A., Conway, A., Blaney, L., 2019. Occurrence and distribution of UV-filters and other anthropogenic contaminants in coastal surface water, sediment, and coral tissue from Hawaii. Sci. Total Environ. 670, 398–410.
- Mladenov, N., Parsons, D., Kinoshita, A.M., Pinongcos, F., Mueller, M., Garcia, D., Lipson, D.A., Grijalva, L.M., Zink, T.A., 2022. Groundwater-surface water interactions and flux of organic matter and nutrients in an urban, Mediterranean stream. Sci. Total Environ. 811, 152379.
- Murphy, K.R., Hambly, A., Singh, S., Henderson, R.K., Baker, A., Stuetz, R., Khan, S.J., 2011. Organic matter fluorescence in municipal water recycling schemes: toward a unified PARAFAC model. Environ. Sci. Technol. 45 (7), 2909–2916.
- Murphy, K.R., Stedmon, C.A., Graeber, D., Bro, R., 2013. Fluorescence spectroscopy and multi-way techniques. PARAFAC. Analyt. Methods 5 (23), 6557–6566.
- Murphy, K.R., Stedmon, C.A., Wenig, P., Bro, R., 2014. OpenFluor– an online spectral library of auto-fluorescence by organic compounds in the environment. Analyt. Methods 6 (3), 658–661.
- Ogidan, O., Giacomoni, M., 2016. Multiobjective genetic optimization approach to identify pipe segment replacements and inline storages to reduce sanitary sewer overflows. Water Res. Manag. 30 (11), 3707–3722.
- Oppenheimer, J., Eaton, A., Badruzzaman, M., Haghani, A.W., Jacangelo, J.G., 2011.
 Occurrence and suitability of sucralose as an indicator compound of wastewater loading to surface waters in urbanized regions. Water Res. 45 (13), 4019–4027.
- Osburn, C.L., Handsel, L.T., Mikan, M.P., Paerl, H.W., Montgomery, M.T., 2012. Fluorescence tracking of dissolved and particulate organic matter quality in a river-dominated estuary. Environ. Sci. Technol. 46 (16), 8628–8636.
- Osburn, C.L., Oviedo-Vargas, D., Barnett, E., Dierick, D., Oberbauer, S.F., Genereux, D.P., 2018. Regional groundwater and storms are hydrologic controls on the quality and export of dissolved organic matter in two tropical rainforest streams, costa rica. J. Geophys. Res.: Biogeosci. 123 (3), 850–866.

Peleato, N.M., McKie, M., Taylor-Edmonds, L., Andrews, S.A., Legge, R.L., Andrews, R.C., 2016. Fluorescence spectroscopy for monitoring reduction of natural organic matter and halogenated furanone precursors by biofiltration. Chemosphere 153, 155–161.

- Ramage, S., Camacho-Muñoz, D., Petrie, B., 2019. Enantioselective LC-MS/MS for anthropogenic markers of septic tank discharge. Chemosphere 219, 191–201.
- Reay, W.G., 2004. Septic tank impacts on ground water quality and nearshore sediment nutrient flux. Groundwater 42 (7), 1079–1089.
- Retelletti Brogi, S., Balestra, C., Casotti, R., Cossarini, G., Galletti, Y., Gonnelli, M., Vestri, S., Santinelli, C, 2020. Time resolved data unveils the complex DOM dynamics in a Mediterranean river. Sci. Total Environ. 733, 139212.
- Retelletti Brogi, S., Jung, J.Y., Ha, S.-Y., Hur, J, 2019. Seasonal differences in dissolved organic matter properties and sources in an Arctic fjord: implications for future conditions. Sci. Total Environ. 694, 133740.
- Rieckermann, J., Bareš, V., Kracht, O., Braun, D., Gujer, W., 2007. Estimating sewer leakage from continuous tracer experiments. Water Res. 41 (9), 1960–1972.
- Roldin, M., Fryd, O., Jeppesen, J., Mark, O., Binning, P.J., Mikkelsen, P.S., Jensen, M.B., 2012. Modelling the impact of soakaway retrofits on combined sewage overflows in a 3km2 urban catchment in Copenhagen, Denmark. J. Hydrol. (Amst) 452-453, 64-75
- Rutsch, M., Rieckermann, J., Krebs, P., 2006. Quantification of sewer leakage: a review. Water Sci. Technol. 54 (6–7), 135–144.
- Sercu, B., Van De Werfhorst, L.C., Murray, J.L.S., Holden, P.A., 2011. Sewage exfiltration as a source of storm drain contamination during dry weather in urban watersheds. Environ. Sci. Technol. 45 (17), 7151–7157.
- Sgroi, M., Roccaro, P., Korshin, G.V., Vagliasindi, F.G.A., 2017. Monitoring the behavior of emerging contaminants in wastewater-impacted rivers based on the use of fluorescence excitation emission matrixes (EEM). Environ. Sci. Technol. 51 (8), 4306–4316.
- Shields, C.A., Band, L.E., Law, N., Groffman, P.M., Kaushal, S.S., Savvas, K., Fisher, G.T., Belt, K.T., 2008. Streamflow distribution of non-point source nitrogen export from urban-rural catchments in the Chesapeake Bay watershed. Water Resour. Res. 44 (9), 1–13
- Singh, S., D'Sa, E.J., Swenson, E.M., 2010. Chromophoric dissolved organic matter (CDOM) variability in Barataria Basin using excitation–emission matrix (EEM) fluorescence and parallel factor analysis (PARAFAC). Sci. Total Environ. 408 (16), 3211–3222.
- Spoelstra, J., Schiff, S.L., Brown, S.J., 2020. Septic systems contribute artificial sweeteners to streams through groundwater. J. Hydrol. X 7, 100050.

- Strahler, A.N., 1957. Quantitative analysis of watershed geomorphology. Eos, Trans. Am. Geophys. Union 38 (6), 913–920.
- Thorndahl, S., Balling, J.D., Larsen, U.B.B., 2016. Analysis and integrated modelling of groundwater infiltration to sewer networks. Hydrol. Process. 30 (18), 3228–3238.
- Topolski, M., 2021. Number of Septic Systems Per HUC-12 in Maryland. Maryland Department of Natural Resources, Annapolis, MD.
- US EPA (2022) United States environmental protection agency, Sanitary Sewer Overflows (SSOs). National pollutant discharge elimination system. Available at https://www.epa.gov/npdes/sanitary-sewer-overflows-ssos. Updated on June 21, 2022
- Wells, C., 2015. Sewer Leak Spills 32,000 Gallons of Sewage Into the Jones Falls. The Baltimore Sun, Baltimore, MD.
- Withers, P.J.A., Jarvie, H.P., Stoate, C., 2011. Quantifying the impact of septic tank systems on eutrophication risk in rural headwaters. Environ. Int. 37 (3), 644–653.
- Withers, P.J.A., May, L., Jarvie, H.P., Jordan, P., Doody, D., Foy, R.H., Bechmann, M., Cooksley, S., Dils, R., Deal, N., 2012. Nutrient emissions to water from septic tank systems in rural catchments: uncertainties and implications for policy. Environ. Sci. Policy 24, 71–82.
- Wu, F.C., Evans, R.D., Dillon, P.J., 2003. Separation and characterization of NOM by high-performance liquid chromatography and on-line three-dimensional excitation emission matrix fluorescence detection. Environ. Sci. Technol. 37 (16), 3687–3693.
- Wu, G., Miao, Z., Shao, S., Jiang, K., Geng, Y., Li, D., Liu, H., 2018. Evaluating the construction efficiencies of urban wastewater transportation and treatment capacity: evidence from 70 megacities in China. Res., Conserv. Recycl. 128, 373–381.
- Wünsch, U.J., Murphy, K.R., Stedmon, C.A., 2017. The one-sample PARAFAC approach reveals molecular size distributions of fluorescent components in dissolved organic matter. Environ. Sci. Technol. 51 (20), 11900–11908.
- Yang, X., Chen, F., Meng, F., Xie, Y., Chen, H., Young, K., Luo, W., Ye, T., Fu, W., 2013. Occurrence and fate of PPCPs and correlations with water quality parameters in urban riverine waters of the Pearl River Delta, South China. Environ. Sci. Pollut. Res. 20 (8), 5864–5875.
- Yu, H., Liang, H., Qu, F., Han, Z.-s., Shao, S., Chang, H., Li, G., 2015. Impact of dataset diversity on accuracy and sensitivity of parallel factor analysis model of dissolved organic matter fluorescence excitation-emission matrix. Sci. Rep. 5 (1), 10207.
- Yuan, D., Zhao, Y., Guo, X., Zhai, L., Wang, X., Wang, J., Cui, Y., He, L., Yan, C., Kou, Y., 2020. Impact of hydrophyte decomposition on the changes and characteristics of dissolved organic matter in lake water. Ecol. Indic. 116, 106482.